

HELAC-Onia: an automatic matrix element generator for heavy quarkonium physics

Hua-Sheng Shao

Department of Physics and State Key Laboratory of Nuclear Physics and Technology,
Peking University, Beijing 100871, China
PH Department, TH Unit, CERN, CH-1211 Geneva 23, Switzerland
E-mail: erdissshaw@gmail.com

ABSTRACT

By the virtues of the Dyson-Schwinger equations, we upgrade the published code HELAC to be capable to calculate the heavy quarkonium helicity amplitudes in the framework of NRQCD factorization, which we dub HELAC-Onia. We rewrote the original HELAC to make the new program be able to calculate helicity amplitudes of multi P-wave quarkonium states production at hadron colliders and electron-positron colliders by including new P-wave off-shell currents. Therefore, besides the high efficiencies in computation of multi-leg processes within the Standard Model, HELAC-Onia is also sufficiently numerical stable in dealing with P-wave quarkonia (e.g. $h_{c,b}$, $\chi_{c,b}$) and P-wave color-octet intermediate states. To the best of our knowledge, it is a first general-purpose automatic quarkonium matrix elements generator based on recursion relations on the market.

arXiv:1212.5293v3 [hep-ph] 27 Aug 2013

PROGRAM SUMMARY

Program title:

HELAC-Onia.

Catalogue number:

Program obtainable from:

<http://helac-phegas.web.cern.ch/helac-phegas>

Licensing provisions: none

Operating system under which the program has been tested:

Windows, Unix.

Programming language:

FORTRAN 90

Keywords:

quarkonium helicity amplitudes, NRQCD, Dyson-Schwinger equations, off-shell currents.

Nature of physical problem:

An important way to explore the law of the nature is to investigate the heavy quarkonium physics at B factories and hadron colliders. However, its production mechanism is still unclear, though NRQCD can explain its decay mechanism in a sufficiently satisfactory manner. The substantial K-factor in heavy quarkonium production processes also implies that the associated production of quarkonium and a relatively large number of particles may play a crucial role in unveiling its production mechanism.

Method of solution:

A labor-saved and efficient way is to make the tedious amplitudes calculation automatic. Based on a recursive algorithm derived from the Dyson-Schwinger equations, the goal of automatic calculation of heavy quarkonium helicity amplitudes in NRQCD has been achieved. Inheriting from the virtues of the recursion relations with the lower computational cost compared to the traditional Feynman-diagram based method, the multi-leg processes (with or without multi-quarkonia up to P-wave states) at colliders are also accessible.

CPC classification code: 4.4 Feynman Diagrams,11.1 General, High Energy Physics and Computing,11.2 Phase Space and Event Simulation,11.5 Quantum Chromodynamics, Lattice Gauge Theory

Typical running time: It depends on the process that is to be calculated. However, typically, for all of the tested processes, they take from several minutes to tens of minutes.

1 Introduction

Studies of heavy-quarkonium systems, e.g. J/ψ , Υ and B_c , provides an important opportunity to investigate quantum chromodynamics (QCD) at hadronic level with the least artificial non-perturbative input parameters by hands. The fact relies on the non-relativistic property formed by relatively heavy charm and bottom quarks. Theoretically, these meson can be described well by non-relativistic QCD (NRQCD)[1] effective theory with only price that some non-perturbative parameters should be determined in prior. Although, in principle, the number of these parameters are not finite, for majority concerned phenomenology analysis, the number of important parameters are always limited given in velocity scaling rule. They can be determined once for all due to their universality property in the effective theory. In fact, NRQCD was established on a factorization theorem that a perturbative high-energy exchange part and a process-independent low-energy part works well in the production and decay processes of heavy quarkonium. The factorization has been proven rigorously for quarkonium decay to all orders, while the theorem in production processes is still absence of proof beyond two-loops. On the phenomenology side, the inconsistency of NRQCD factorization, cross section and polarization of heavy quarkonium production has not been eliminated yet[2]. Hence, fair to say, the mechanism of heavy quarkonium production is still unclear by now.

The motivation of the paper is to develop an automatic tool for performing investigations in heavy quarkonium physics. Compared to some of the traditional Feynman-diagram based tools[3, 4], the package inherits the abilities of HELAC[5, 6, 7], which is based on a recursive algorithm and hence reduces the computational cost that grows asymptotically as $n!$ to a^n with $a \sim 3$, where n is the number of external legs in the considered process. Therefore, we expect it provides a more efficient way for people to do physical analysis with multi-particle processes, which might be especially important in quarkonium physics[8].

Now we are intending to give a short list of the features in our program compared with MADONIA[3]. Since HELAC-Onia is calculated with the recursion relations, the speed of matrix element calculation is expected to be higher than that by MADONIA. We have tested a simple process $gg \rightarrow c\bar{c}J/\psi(\beta)$. The time in generating one unweighted event by HELAC-Onia is less than that by MADONIA about a factor of 4. Furthermore, HELAC-Onia is quite suitable to calculate multi-quarkonia production, while in MADONIA the number of quarkonium is restricted to be one. In MADONIA, the computation of P-wave amplitude is performing by a numerical derivation, which is expected to be numerical unstable in multi P-wave quarkonia production, while in HELAC-Onia this problem is cured by introducing new P-wave currents which will be described in the following sections. Another advantage in HELAC-Onia is that it is much easier in its use. On the other hand,

because MADONIA is based on Feynman diagrams, it is much more flexible to select some specific diagrams like some diagrams via some specific s-channel propagators, which is difficult to realize in recursion relations. While in HELAC-Onia the feasible processes are only restricted to $pp(\bar{p})$ and e^-e^+ collisions at least now, MADONIA is able to be applied at more colliders as well as subsequent decays.

Before closing this section, we describe the organization of the paper. In section 2, the recursive algorithm in HELAC is revised. In section 3, we demonstrate the strategies in helicity amplitudes calculations of heavy quarkonium production in HELAC-Onia, and especially the description of P-wave off-shell currents. Several benchmark processes are computed in section 4. Finally, we explain our program and draw our conclusions and outlooks in the last two sections respectively.

2 The recursive algorithm

The algorithm of HELAC[5, 6, 7] is based on the Dyson-Schwinger equations[9, 10, 11], which is an generalized version of the Berends-Giele off-shell recursive relation[12]. To illustrate it, we consider a process with n external legs. The momenta of these external legs are denoted as p_1, p_2, \dots, p_n , and the quantum numbers (e.g. color, helicity) are defined by $\alpha_1, \alpha_2, \dots, \alpha_n$. An off-shell current with k external legs can be represented as

$$\mathcal{J}(\{p_{i_1}, \dots, p_{i_k}\}; \{\alpha_{i_1}, \dots, \alpha_{i_k}\}) \equiv \text{Diagram} \quad (1)$$

All of the subgraphs that are able to transfer the k external legs into the off-shell current \mathcal{J} according to the Feynman rules in the considered model have been included into the shade bubble. Every current is assigned by a "level" l , which is defined as the number of external legs involved in the current, i.e. the "level" of $\mathcal{J}(\{p_{i_1}, \dots, p_{i_k}\}; \{\alpha_{i_1}, \dots, \alpha_{i_k}\})$ is k . In special, the "level" of each external leg is 1. Then, in general, all of the currents with higher "level" can be constructed from those with lower "level". The starting point of the recursion relation is from the $l = 1$ currents, i.e. the external legs. For the i -th

external leg, the corresponding current¹ is its wavefunction

$$\mathcal{J}(\{p_i\}; \{\alpha_i\}) \equiv \xrightarrow{p_i, \alpha_i} . \quad (2)$$

Specifically, for a vector boson

$$\mathcal{J}(\{p_i\}; \{\mu, \lambda\}) \equiv \epsilon_\lambda^\mu(p_i), \quad (3)$$

where μ is the lorentz index and λ is the helicity of the vector boson ($\lambda = \pm 1$ for a massless vector, while $\lambda = \pm 1, 0$ for a massive vector)², while for a spin- $\frac{1}{2}$ fermion

$$\begin{aligned} \mathcal{J}(\{p_i\}; \{+1, \lambda\}) &\equiv \begin{cases} u_\lambda(p_i) & \text{when } p_i^0 \geq 0 \\ v_\lambda(-p_i) & \text{when } p_i^0 \leq 0 \end{cases} , \\ \mathcal{J}(\{p_i\}; \{-1, \lambda\}) &\equiv \begin{cases} \bar{u}_\lambda(p_i) & \text{when } p_i^0 \geq 0 \\ \bar{v}_\lambda(-p_i) & \text{when } p_i^0 \leq 0 \end{cases} , \end{aligned} \quad (4)$$

where $+1$ and -1 means fermion flow and anti-fermion flow respectively, λ is the helicity index with $\lambda = \pm 1$. The explicit expressions of these $l = 1$ wavefunctions are presented in the appendix of Ref.[5]. The currents with $l = k > 1$ can be constructed from the currents with lower l ³

$$\begin{aligned} & \text{Diagram with } k \text{ legs } (p_{i_1}, \alpha_1, \dots, p_{i_k}, \alpha_k) \text{ and } P \text{ leg} \\ &= \sum_{\sigma} \sum_{r,s>0}^{r+s=k} \left[\text{Diagram with } r \text{ legs } (p_{i_{\sigma(r)}}, \alpha_{\sigma(r)}) \text{ and } P \text{ leg} \right. \\ & \quad \left. + \text{Diagram with } r+s \text{ legs } (p_{i_{\sigma(r+s)}}, \alpha_{\sigma(r+s)}) \text{ and } P \text{ leg} \right] \\ &+ \sum_{\sigma} \sum_{r,s,t>0}^{r+s+t=k} \left[\text{Diagram with } r \text{ legs } (p_{i_{\sigma(r)}}, \alpha_{\sigma(r)}) \text{ and } P \text{ leg} \right. \\ & \quad \left. + \text{Diagram with } r+s \text{ legs } (p_{i_{\sigma(r+s)}}, \alpha_{\sigma(r+s)}) \text{ and } P \text{ leg} \right. \\ & \quad \left. + \text{Diagram with } r+s+t \text{ legs } (p_{i_{\sigma(r+s+t)}}, \alpha_{\sigma(r+s+t)}) \text{ and } P \text{ leg} \right] , \end{aligned} \quad (5)$$

where σ means to exhaust all possible generating "level" r, s (and t) currents formed by the i_1, \dots, i_k external legs. Each off-shell currents should be multiplied by its propagator. The end of the recursion is the forming of the "level" n current, in which we choose all $l = n - 1$ currents⁴ to multiply with the first external particle's wavefunction. If the flavor

¹The "level" 1 current is on-shell instead of off-shell.

²Note that, for simplicity, we have suppressed other possible quantum numbers like color for gluon.

³For simplicity, we only consider tri-linear and quadri-linear couplings. However, it is straightforward to include higher-point vertices as well.

⁴Actually, they are on-shell instead of off-shell.

of the first external particle is not exactly same as the flavor of the $l = n - 1$ current, the current is dropped. Finally, we obtain the resulting amplitude. In this way, one can avoid computing identical sub-graphs contributing different Feynman diagrams more than once. The summation of the all sub-graphs that contribute to a specific current also reduces the number of objects that should be used in the next "level" recursion formula. Therefore, the computation complexity will be reduced from $\sim n!$ in Feynman-diagram based algorithm to $\sim a^n$ in the Dyson-Schwinger based recursive algorithm, where $a \sim 3$.

In the original HELAC program[5], it uses a binary representation of the momenta involved in the considered process[13]. For each of the external momenta p_1, \dots, p_n , its binary representation is 2^{i-1} for i -th external leg with momenta p_i , while for a $l = k$ current $\mathcal{J}(\{p_{i_1}, \dots, p_{i_k}\}; \{\alpha_{i_1}, \dots, \alpha_{i_k}\})$, it is expressed as $\sum_{j=1}^k 2^{j-1}$. Then, each momentum $P^\mu = \sum_{j=1}^n m_j p_j$ can be uniquely expressed by an integer $m = \sum_{j=1}^n 2^{j-1} m_j$ where $m_j = 0$ or 1. In this case, the "level" of an current with momentum $P^\mu = \sum_{j=1}^n m_j p_j$ can be calculated directly by $l = \sum_{j=1}^n m_j$. In this case, the sign factor from the anti-symmetric property of fermions is obtained by

$$\epsilon(P_1, P_2) = (-1)^{\chi(P_1, P_2)}, \chi(P_1, P_2) = \sum_{i=n}^2 \hat{m}_{1i} \sum_{j=1}^{i-1} \hat{m}_{2j} \quad (6)$$

, with

$$\begin{aligned} P_1 &= \sum_{j=1}^n m_{1j} p_j, \\ P_2 &= \sum_{j=1}^n m_{2j} p_j, \\ \hat{m}_{1j} &= \begin{cases} 0 & \text{when particle } j \text{ is a boson} \\ m_{1j} & \text{when particle } j \text{ is a fermion} \end{cases}, \\ \hat{m}_{2j} &= \begin{cases} 0 & \text{when particle } j \text{ is a boson} \\ m_{2j} & \text{when particle } j \text{ is a fermion} \end{cases}. \end{aligned} \quad (7)$$

If the current is constructed by a tri-linear coupling with the lower "level" currents P_1 and P_2 , it should be multiplied by a factor $\epsilon(P_1, P_2)$. If it is constructed by a quadri-linear coupling with currents P_1, P_2 and P_3 , the sign factor is $\epsilon(P_1, P_2, P_3) = \epsilon(P_1, P_2)\epsilon(P_1 + P_2, P_3)$.

The way of the color treatment is also an interesting topic in the matrix element generator. In HELAC, it is using the widely used color flow basis, which was first proposed in Ref.[14] and was applied in perturbative QCD computations in Refs.[15, 16]. Basically, a color octet gluon field A_μ^a is replaced by a 3×3 matrix $(\mathcal{A}_\mu)_j^i = \frac{1}{\sqrt{2}} A_\mu^a (\lambda^a)_j^i$, where λ^a is

the Gell-Mann matrix, i.e. $\mathbf{8} = \mathbf{3} \otimes \bar{\mathbf{3}} - \mathbf{1}$, while incoming quarks or outgoing antiquarks still maintain in the $\mathbf{3}$ representation of SU(3) and outgoing quarks or incoming antiquarks are in $\bar{\mathbf{3}}$ representation. After this substitution, only the Kronecker notation δ s appear in the Feynman rules. All the Feynman rules in the color-flow basis have been established in Ref.[16]. If there are n_g external gluons (denote as $1, 2, \dots, n_g$) and n_q external quark-antiquark pairs (denote as $n_g + 1, n_g + 2, \dots, n_g + n_q$) in the considered process, the color basis for the amplitude will be in the form of

$$\mathcal{C}_i = \delta_{\sigma_i(1)}^1 \cdots \delta_{\sigma_i(n_g+n_q)}^{n_g+n_q}, \quad (8)$$

where σ_i represents the i -th permutation of $1, 2, \dots, n_g + n_q$. There are totally $(n_g + n_q)!$ color basis, though some of them will vanish. With this basis, one can construct the color matrix via

$$M_{ij} = \sum \mathcal{C}_i \mathcal{C}_j^*, \quad (9)$$

and obtain the final square of matrix elements by

$$|\mathcal{M}|^2 = \sum_{i,j=1}^{(n_g+n_q)!} A_i M_{ij} A_j^*, \quad (10)$$

where A_i and A_j are the color-stripped amplitudes.

In order to improve the computation efficiency, a Monte Carlo sampling over the helicity configurations is adopted in the program[5] to perform the helicity summation. The basic idea of this technology is simple. Let us take a massive vector boson for example. A massive vector boson has three helicity states $\lambda = \pm 1, 0$ with wavefunctions $\epsilon_+^\mu, \epsilon_-^\mu, \epsilon_0^\mu$. The strategy puts the concrete helicity summation of $\sum_{\lambda=\pm,0} \epsilon_\lambda^\mu (\epsilon_\lambda^\nu)^*$ into a continue integration by defining $\epsilon_\phi^\mu \equiv \sum_{\lambda=\pm,0} e^{i\lambda\phi} \epsilon_\lambda^\mu$. Then, the summation becomes $\int_0^{2\pi} d\phi \epsilon_\phi^\mu (\epsilon_\phi^\nu)^*$, which can be calculated easily by a Monte Carlo program.

3 Quarkonium amplitudes in NRQCD

In the framework of the NRQCD factorization, the cross section of a heavy quarkonium production can be written as a combination of the perturbative short-distance parts and the non-perturbative long-distance matrix elements. For example at the proton-proton collider, the factorized form of a heavy quarkonium \mathcal{Q} production is written as

$$\sigma(pp \rightarrow \mathcal{Q} + X) = \sum_{i,j,n} \int dx_1 dx_2 f_{i/p}(x_1) f_{j/p}(x_2) \hat{\sigma}(ij \rightarrow Q\bar{Q}[n] + X) \langle \mathcal{O}_n^{\mathcal{Q}} \rangle, \quad (11)$$

where $f_{i/p}$ and $f_{j/p}$ are the parton distribution functions, $\hat{\sigma}(ij \rightarrow Q\bar{Q}[n] + X)$ is the short distance cross section of producing a heavy quark pair $Q\bar{Q}$ in a specific quantum state

n , and $\langle \mathcal{O}_n^{\mathcal{Q}} \rangle$ represents as the long distance matrix element. In principle, for a specific quarkonium \mathcal{Q} , there are infinity number of Fock states n and infinity number of long distance matrix elements $\langle \mathcal{O}_n^{\mathcal{Q}} \rangle$. The power counting rules in NRQCD tell us for any quarkonium, there are only limited Fock states should be involved in our calculations up to a specific order of v , where v is the relative velocity of the heavy quark pair that forms the quarkonium. It makes NRQCD be predictable for hadrons. For example, in the process of J/ψ production, there are only four different Fock states (i.e. β , $^3S_1^{[8]}$, $^3P_J^{[8]}$ and $^1S_0^{[8]}$)⁵ contributing to its cross section up to v^7 . The color-singlet long distance matrix element can be estimated from the phenomenological models like potential models, while the color-octet long distance matrix elements can only be determined from the experimental data till now.

3.1 Projection method

To evaluate the process-dependent short distance coefficients, one has to constraint the $Q\bar{Q}$ into a specific quantum state. A convenient way to do it is performing projection.

Specifically, the color projectors to the process $ij \rightarrow Q\bar{Q}[^{2S+1}L_J^{[c]}] + X$ are [17] $\frac{\delta_{ij}}{N_c}$ when $c = 1$ and $\sqrt{2}\lambda_{ij}^a$ when $c = 8$, where i, j are the color indices of the heavy quark pair $Q\bar{Q}$ and λ^a is the Gell-Mann matrix. The color octet projector which contains the Gell-Mann matrix will be decomposed into the color-flow basis in the HELAC-Onia. Moreover, after projecting, no color indices of the heavy quark pair in the color-singlet states will appear.

Another important constraint of the heavy quark pair is their total spin. The spin projectors were first derived in Refs.[18, 19]. The general form of the projectors is⁶

$$-\frac{1}{2\sqrt{2}(E+m_Q)}\bar{v}(p_2, \lambda_2)\Gamma_S\frac{\not{P}+2E}{2E}u(p_1, \lambda_1), \quad (12)$$

where m_Q is the mass of the heavy quark, p_1, p_2 and λ_1, λ_2 are the heavy quarks' momenta and helicity respectively, $P^\mu = p_1^\mu + p_2^\mu$ is the total momentum of the heavy quark pair and $E = \frac{\sqrt{P^2}}{2}$. The Γ_S is γ_5 when $S = 0$, and it is $\epsilon_\mu^{\lambda_s}\gamma^\mu$ when $S = 1$, where $\lambda_s = \pm, 0$ is the helicity of the quarkonium \mathcal{Q} and $\epsilon_\mu^{\lambda_s}$ is the polarization vector for the spin triplet state. For S-wave and P-wave states without relativistic corrections, E can be set as m_Q directly. After applying the spin projection, the two external wavefunctions for open

⁵We write the Fock states in the spectroscopic form of $n = ^{2S+1}L_J^{[c]}$, where S, L, J identify the spin, orbital momentum, total angular momentum states respectively, and $c = 1, 8$ means that the intermediate state $Q\bar{Q}$ can be in color-singlet or color-octet state.

⁶In HELAC-Onia, we also generalize the projectors in the case of the heavy quarks in different flavors that form a heavy quarkonium like B_c . But for simplicity, we only consider the same flavor case here.

Q and \bar{Q} will be glued. It results in a problem in the recursive relation, because the recursion begins from the external wavefunctions. In order to cure it, we decide to cut the glued fermion chain at the place of $\not{P} + 2E$ in the projector Eq.(12). Using the completeness relation of $\not{P} + 2E = \sum_{\lambda'=\pm} u(P, \lambda')\bar{u}(P, \lambda')$, we use the new "wavefunction" for Q as $\frac{1}{m_Q}\bar{u}(P, \lambda')(\not{p}_1 + m_Q)$ and for \bar{Q} as $-\frac{1}{8\sqrt{2}m_Q}(\not{p}_2 - m_Q)u(P, \lambda')$. Considering the λ' in the "wavefunctions" of Q and \bar{Q} should be exactly same, we have to perform the direct summation of λ' in stead of Monte Carlo sampling in the HELAC-0nia.

3.2 P-wave currents in HELAC-0nia

The P-wave calculations are always necessary in the NRQCD predictions for both P-wave states $h_{c/b}, \chi_{c/b}$ and S-wave states $J/\psi, \Upsilon, \eta_{c/b}$. For example, the color-octet P-wave states ${}^3P_J^{[8]}$ are playing special roles in J/ψ hadroproduction[20, 21, 22, 23, 24] and photoproduction[25, 26]. Although they are power suppressed in NRQCD compared to β , fragmentation topologies make them overwhelming the color-singlet one at the medium and high transverse momentum regime. Hence, HELAC-0nia is designed to be able to handle with P-wave states as well with a numerical stable method by introducing new P-wave off-shell currents.

After expanding the relative momentum $q^\nu = \frac{p_1^\nu - p_2^\nu}{2}$ between the heavy quark pair in the amplitude $\mathcal{A}(ij \rightarrow Q(p_1)\bar{Q}(p_2) + X)$ in the non-relativistic approximation, the formula for the calculation of P-wave amplitude is

$$(\epsilon_\nu^{\lambda_l})^* \frac{\partial}{\partial q_\nu} \mathcal{A}(ij \rightarrow Q(p_1)\bar{Q}(p_2) + X) \Big|_{q=0}, \quad (13)$$

where $\lambda_l = \pm, 0$ is the helicity configuration of the polarization vector $\epsilon_\nu^{\lambda_l}$ for P-wave state. The treatment of the new "wavefunctions" definition of the heavy quark pair avoids the derivation of the spinors, which might result in numerical instability.

Alternatively, one could also do a direct numerical derivation by keeping the small relative momentum q of the quark and antiquark that forms the heavy quarkonium and approaching q to zero in the quarkonium rest frame[3]. However, this direct numerical derivation might result in numerical unstable potentially especially when there are many P-wave states involved in the process.

In contrast, the P-wave currents, which are extended from the original off-shell currents at parton level, can be written in a much compact manner. In the HELAC-0nia, we assign each current with an derivation index, which is also in binary representation. Assuming there are n_P P-wave states in the considered process, the relative momenta of the i -th heavy quark pair that forms P-wave state is denoted as q_i where $i = 1, \dots, n_P$. The

general derivation index form for a current is $b = \sum_{i=1}^{n_P} b_i 2^{i-1}$ with $b_i = 0$ or 1 . If the current has been derived by q_i as done like in Eq.(13), b_i is 1 , otherwise $b_i = 0$. Finally, only the amplitudes with $b = 2^{n_P} - 1$ are kept. The numerical stable form of P-wave currents avoids the large numerical cancellation.

4 Benchmark processes

We are in the position to illustrate the validation and applications of HELAC-Onia to the heavy quarkonium production at the proton-proton, proton-antiproton and electron-positron colliders.

4.1 B_c meson production at the LHC

B_c production is an interesting channel to investigate QCD, and it has been widely studied at the hadron colliders[27, 28, 29]. The available results have been used by the MADONIA[3] for testing the correctness of the code. We will also compare our results calculated by the HELAC-Onia with those presented in Ref.[3]. We only consider the B_c production at the LHC with the center-of-mass energy 14 TeV with the initial gluon-gluon fusion and quark-antiquark annihilation here. All of the input parameters are taken as same as those in Ref.[3]:

- (1) The masses of the bottom, charm quarks and B_c meson are set as $m_b = 4.9$ GeV, $m_c = 1.5$ GeV, $m_{B_c} = m_b + m_c = 6.4$ GeV.
- (2) The parton distribution function (PDF) set is chosen as CTEQ6L1 [30].
- (3) The factorization scale μ_F of PDF and the renormalization scale μ_R are set as $\mu_F = \mu_R = 2(m_b + m_c) = 12.8$ GeV. Moreover, the strong coupling constant is fixed as $\alpha_S(\mu_R) = 0.189$.
- (4) The color-singlet long distance matrix elements are taken as $\langle \mathcal{O}^{B_c}(^{2S+1}S_J^{[1]}) \rangle = (2J+1)0.736$ GeV³, $\langle \mathcal{O}^{B_c}(^{2S+1}P_J^{[1]}) \rangle = (2J+1)0.287$ GeV⁵.
- (5) The color-octet long distance matrix elements are related with the color-singlet ones, i.e. $\langle \mathcal{O}^{B_c}(^{2S+1}S_J^{[8]}) \rangle = \langle \mathcal{O}^{B_c}(^{2S+1}S_J^{[1]}) \rangle / 100$, $\langle \mathcal{O}^{B_c}(^{2S+1}P_J^{[8]}) \rangle = \langle \mathcal{O}^{B_c}(^{2S+1}P_J^{[1]}) \rangle / 100$.

Our final results (with Monte Carlo statistical errors) are shown in the second column of Table.1, where we also listed the corresponding results (in the third column of Table.1) presented in Ref.[3] for the convenience of comparison. We find that our results are in agreement with those in Ref.[3].

process	HELAC-Onia(nb)	MADONIA(nb)
$gg \rightarrow B_c^+(^1S_0^{[1]})b\bar{c}$	39.3994 ± 0.0958382	39.4
$gg \rightarrow B_c^+(^3S_1^{[1]})b\bar{c}$	98.3109 ± 0.287252	98.3
$gg \rightarrow B_c^+(^1P_1^{[1]})b\bar{c}$	5.21131 ± 0.0144431	5.20
$gg \rightarrow B_c^+(^3P_J^{[1]})b\bar{c}$	16.7341 ± 0.0589108	16.72
$gg \rightarrow B_c^+(^1S_0^{[8]})b\bar{c}$	0.411671 ± 0.00169734	0.411
$gg \rightarrow B_c^+(^3S_1^{[8]})b\bar{c}$	1.78657 ± 0.00624756	1.79
$gg \rightarrow B_c^+(^1P_1^{[8]})b\bar{c}$	0.11816 ± 0.000754526	0.117
$gg \rightarrow B_c^+(^3P_J^{[8]})b\bar{c}$	0.305862 ± 0.0011841	0.3051
$q\bar{q} \rightarrow B_c^+(^1S_0^{[1]})b\bar{c}$	0.137782 ± 0.000896985	0.137
$q\bar{q} \rightarrow B_c^+(^3S_1^{[1]})b\bar{c}$	0.83905 ± 0.00524885	0.834
$q\bar{q} \rightarrow B_c^+(^1P_1^{[1]})b\bar{c}$	$0.0296125 \pm 0.000154919$	0.0295
$q\bar{q} \rightarrow B_c^+(^3P_J^{[1]})b\bar{c}$	0.111259 ± 0.000839535	0.1105
$q\bar{q} \rightarrow B_c^+(^1S_0^{[8]})b\bar{c}$	$0.00103294 \pm 4.44716 \cdot 10^{-6}$	0.00103
$q\bar{q} \rightarrow B_c^+(^3S_1^{[8]})b\bar{c}$	$0.00707624 \pm 0.0000459292$	0.00703
$q\bar{q} \rightarrow B_c^+(^1P_1^{[8]})b\bar{c}$	$0.000253678 \pm 2.19206 \cdot 10^{-6}$	0.000251
$q\bar{q} \rightarrow B_c^+(^3P_J^{[8]})b\bar{c}$	$0.000826534 \pm 5.16988 \cdot 10^{-6}$	0.0008207

Table 1: Cross sections of inclusive B_c^+ production at the LHC with the center-of-mass energy 14 TeV. The data in the third column are taken from Ref.[3]. In the second column, the Monte Carlo statistical errors are also given.

4.2 Charmonia production at the B factory

The charmonia production from the electron-positron collisions has been extensively studied over the past decade. We do not intend to recall the long story of the theoretical and experimental studies on this topic here, which was already summarized in Ref.[31]. We only want to show the application and validation of the program HELAC-Onia in calculating the quarkonium observables in the e^+e^- colliders in this section.

The first theoretical results of the inclusive charmonium association production with $c\bar{c}$ via single virtual photon exchanging at the B factory with the center-of-mass energy 10.6 GeV was presented in Ref.[32], which are only calculated at the leading order in α_S and v . Moreover, the results of η_c and J/ψ production with gluons at the B factory are given in Ref.[3]. We put the same input parameters into HELAC-Onia:

- (1) The charm quark's mass m_c is 1.5 GeV, and the masses of the charmonia considered are $2m_c = 3$ GeV. The mass of the electron and positron are safely ignored.

- (2) The renormalization scale μ_R is chosen as $2m_c = 3$ GeV. In this way, the strong coupling constant is fixed as $\alpha_S(\mu_R) = 0.26$, while the electromagnetic fine structure constant is also set as $\alpha = 1/137$.
- (3) The color-singlet long distance matrix elements are $\langle \mathcal{O}^{(2S+1)S_J^{[1]}} \rangle = (2J+1)0.387 \text{ GeV}^3$.

Our color-singlet S-wave results are presented in Table.2, from which we see that all of our results are in good agreement with those in Refs.[32, 3]. In the first two rows of Table.4, we also presented the cross sections of η_c and J/ψ production in association with $c\bar{c}$ at $\mathcal{O}(\alpha^2\alpha_S^2 + \alpha^3\alpha_S + \alpha^4)$, which means that we have include both the single photon exchanging channel and the double photon exchanging channel. To the best of our knowledge, they are new.

Several years ago, it was reported that there was a large discrepancy between the theoretical predictions and the experimental measurements in the exclusive double charmonia production at the B factory (see review in e.g.Ref.[31]). The large discrepancy has attracted a lot of studies in this fields. We recalculated some of the cross sections at the B factory with $\sqrt{s} = 10.6$ GeV in Table.3 with the same input as those given in Ref.[33]. We listed the input parameters as following:

- (1) The mass of the charm quark is 1.4 GeV, and the masses of the charmonia are $2m_c$.
- (2) The renormalization scale μ_R is set as $\sqrt{s}/2 = 5.3$ GeV, and $\alpha_S(\mu_R) = 0.21, \alpha = 1/137$.
- (3) The color-singlet long distance matrix elements are $\langle \mathcal{O}^{(2S+1)S_J^{[1]}} \rangle = (2J+1)0.335 \text{ GeV}^3$ and $\langle \mathcal{O}^{(2S+1)P_J^{[1]}} \rangle = (2J+1)0.053 \text{ GeV}^5$.

The results in Table.3 only include $\mathcal{O}(\alpha^2\alpha_S^2)$ and leading-order in v perturbative calculations. Good agreement is found between HELAC-Onia and Ref.[33]. The $\mathcal{O}(\alpha^2\alpha_S^2 + \alpha^3\alpha_S + \alpha^4)$ cross sections for $J/\psi J/\psi$ and $J/\psi h_c$ exclusive productions are shown in the last two rows of Table.4. These results agree with those given in Ref.[34].

4.3 Double quarkonia production at the Tevatron and the LHC

Double quarkonia production at the hadron colliders is a useful way to investigate the color-octet mechanism. In this section, we will compare the results calculated by HELAC-Onia and those in the literature[35]. The input parameters (same as those in Ref.[35]) are:

- (1) $m_c = 1.5, m_b = 4.9$. The mass of a heavy quarkonium is just approximated as the sum of its constituent heavy quarks' masses. In other words, if a heavy quarkonium H is composed by $Q_1\bar{Q}_2$, then $m_H = m_{Q_1} + m_{Q_2}$.

process	HELAC-Onia(fb)	Refs.[32, 3](fb)
$e^+e^- \rightarrow \gamma^* \rightarrow \eta_c(^1S_0^{[1]})c\bar{c}$	58.7938 ± 0.154193	58.7
$e^+e^- \rightarrow \gamma^* \rightarrow \eta_c(^1S_0^{[1]})ggg$	3.72893 ± 0.0063512	3.72
$e^+e^- \rightarrow \gamma^* \rightarrow J/\psi(^3S_1^{[1]})c\bar{c}$	147.864 ± 0.305001	148
$e^+e^- \rightarrow \gamma^* \rightarrow J/\psi(^3S_1^{[1]})gg$	266.037 ± 0.247366	266

Table 2: Cross sections of the inclusive η_c and J/ψ production via single virtual photon exchanging at the B factory with the center-of-mass energy 10.6 GeV.

process	HELAC-Onia(fb)	Ref.[33](fb)
$e^+e^- \rightarrow \gamma^* \rightarrow J/\psi(^3S_1^{[1]})\eta_c(^1S_0^{[1]})$	3.78154 ± 0.00338108	3.78
$e^+e^- \rightarrow \gamma^* \rightarrow h_c(^1P_1^{[1]})\eta_c(^1S_0^{[1]})$	0.308533 ± 0.000198459	0.308
$e^+e^- \rightarrow \gamma^* \rightarrow J/\psi(^3S_1^{[1]})\chi_{cJ}(^3P_J^{[1]})$	3.47635 ± 0.00453553	3.47
$e^+e^- \rightarrow \gamma^* \rightarrow h_c(^1P_1^{[1]})\chi_{cJ}(^3P_J^{[1]})$	0.328299 ± 0.000392734	0.328

Table 3: Cross sections of the exclusive double charmonia production via single virtual photon exchanging at the B factory with the center-of-mass energy 10.6 GeV.

process	HELAC-Onia(fb)	Ref.[34](fb)
$e^+e^- \rightarrow \eta_c(^1S_0^{[1]})c\bar{c}$	61.6802 ± 0.0854359	—
$e^+e^- \rightarrow J/\psi(^3S_1^{[1]})c\bar{c}$	166.499 ± 0.175318	—
$e^+e^- \rightarrow J/\psi(^3S_1^{[1]})J/\psi(^3S_1^{[1]})$	6.64805 ± 0.0123474	6.65
$e^+e^- \rightarrow J/\psi(^3S_1^{[1]})h_c(^1P_1^{[1]})$	$0.00606923 \pm 6.84416 \cdot 10^{-6}$	0.0061

Table 4: The $\mathcal{O}(\alpha^2\alpha_S^2 + \alpha^3\alpha_S + \alpha^4)$ cross sections of the charmonia production at the B factory with the center-of-mass energy 1.96 GeV.

Final States	HELAC-Onia(nb)	Ref.[35](nb)
$2\eta_c(^1S_0^{[1]})$	$3.316 \cdot 10^{-3} \pm 3.705 \cdot 10^{-6}$	$3.32 \cdot 10^{-3}$
$2J/\psi(^3S_1^{[1]})$	$0.05631 \pm 4.437 \cdot 10^{-5}$	0.0563
$2\eta_b(^1S_0^{[1]})$	$1.866 \cdot 10^{-5} \pm 2.385 \cdot 10^{-8}$	$1.87 \cdot 10^{-5}$
$2\Upsilon(^3S_1^{[1]})$	$1.226 \cdot 10^{-4} \pm 1.489 \cdot 10^{-7}$	$1.23 \cdot 10^{-4}$
$B_c(^1S_0^{[1]})\bar{B}_c(^1S_0^{[1]})$	$3.854 \cdot 10^{-3} \pm 9.529 \cdot 10^{-6}$	$3.86 \cdot 10^{-3}$
$B_c(^1S_0^{[1]})\bar{B}_c(^3S_1^{[1]})$	$1.001 \cdot 10^{-3} \pm 2.492 \cdot 10^{-6}$	$1.00 \cdot 10^{-3}$
$B_c(^3S_1^{[1]})\bar{B}_c(^3S_1^{[1]})$	$8.226 \cdot 10^{-3} \pm 9.531 \cdot 10^{-6}$	$8.23 \cdot 10^{-3}$

Table 5: Cross sections of double quarkonium production at the Tevatron with the center-of-mass energy 1.96 TeV.

- (2) $\mu_F = \mu_R = \sqrt{m_H^2 + p_T^2}$ for the heavy quarkonium H .
- (3) PDF set is CTEQ6L1 [30]. Therefore, the running of α_S is evaluated by the leading-order formula in the PDF set.
- (4) The S-wave color-singlet long distance matrix elements are $\langle \mathcal{O}^{c\bar{c}}(^{2S+1}S_J^{[1]}) \rangle = (2J+1)0.389134 \text{ GeV}^3$, $\langle \mathcal{O}^{b\bar{b}}(^{2S+1}S_J^{[1]}) \rangle = (2J+1)2.34722 \text{ GeV}^3$ and $\langle \mathcal{O}^{b\bar{c}}(^{2S+1}S_J^{[1]}) \rangle = (2J+1)0.720017 \text{ GeV}^3$.
- (5) The pseudorapidity η cuts on the final quarkonia are $|\eta| < 0.6$ at the Tevatron and $|\eta| < 2.4$ at the LHC.

The S-wave color-singlet cross sections are shown in Table.5 (Tevatron with $\sqrt{s} = 1.96 \text{ TeV}$) and in Table.6 (LHC with $\sqrt{s} = 14 \text{ TeV}$).

4.4 Hadroproduction of J/ψ and Υ in association with a heavy-quark pair

The measurements of the J/ψ and Υ in association with a heavy quark pair at the hadron collider are interesting because not only they will contribute to the inclusive J/ψ and Υ production but also they are useful way to study color-octet mechanism at the Tevatron and the LHC. In figure 1, we present the transverse momentum p_T distributions of J/ψ and Υ via color-singlet channel at the Tevatron with $\sqrt{s} = 1.96 \text{ TeV}$ and the LHC with $\sqrt{s} = 14 \text{ TeV}$. All of our results are in agreement with those in Ref.[36]. For completeness, we list our input for calculation $J/\psi c\bar{c}$ and $\Upsilon b\bar{b}$ production as follows:

Final States	HELAC-Onia(nb)	Ref.[35](nb)
$2\eta_c(^1S_0^{[1]})$	2.730 ± 0.01710	2.73
$2J/\psi(^3S_1^{[1]})$	$2.832 \pm 1.721 \cdot 10^{-3}$	2.83
$2\eta_b(^1S_0^{[1]})$	$7.373 \cdot 10^{-3} \pm 1.802 \cdot 10^{-5}$	$7.36 \cdot 10^{-3}$
$2\Upsilon(^3S_1^{[1]})$	$0.01514 \pm 1.184 \cdot 10^{-5}$	0.0151
$B_c(^1S_0^{[1]})\bar{B}_c(^1S_0^{[1]})$	$0.2723 \pm 1.461 \cdot 10^{-4}$	0.272
$B_c(^1S_0^{[1]})\bar{B}_c(^3S_1^{[1]})$	$0.08379 \pm 4.430 \cdot 10^{-5}$	0.0837
$B_c(^3S_1^{[1]})\bar{B}_c(^3S_1^{[1]})$	$0.7078 \pm 3.797 \cdot 10^{-4}$	0.708

Table 6: Cross sections of double quarkonium production at the LHC with the center-of-mass energy 14 TeV.

- (1) $m_c = 1.5$ GeV, $m_b = 4.75$ GeV and $m_{J/\psi} = 2m_c, m_\Upsilon = 2m_b$.
- (2) $\mu_F = \mu_R = \sqrt{(4m_Q)^2 + p_T^2}$, where m_Q is m_c for $J/\psi c\bar{c}$ and m_b for $\Upsilon b\bar{b}$.
- (3) PDF set is CTEQ6M [30]. The running of α_S is following the next-to-leading order formula in CTEQ.
- (4) The color-singlet long distance matrix elements are $\langle \mathcal{O}^{J/\psi}(\beta) \rangle = 1.16024$ GeV³ and $\langle \mathcal{O}^\Upsilon(\beta) \rangle = 9.28192$ GeV³.
- (5) The rapidity cuts are applied as $|y| < 0.6$ at the Tevatron and $|y| < 0.5$ at the LHC.

4.5 Spin density matrix and polarization

Besides the total cross sections and other unpolarized observables like p_T spectrum, HELAC-Onia is also designed to be able to calculate the spin density matrices of heavy quarkonia. Hence, it can be taken as a useful tool to calculate the polarization observables of heavy quarkonia in various polarization frames. It has been successfully used in:

- (1) the next-to-leading order inclusive J/ψ polarization at the Tevatron and LHC [23];
- (2) the polarization of the inclusive χ_c hadroproduction [37, 38];
- (3) the polarized χ_c production in associate with a charm quark pair at the LHC[39].

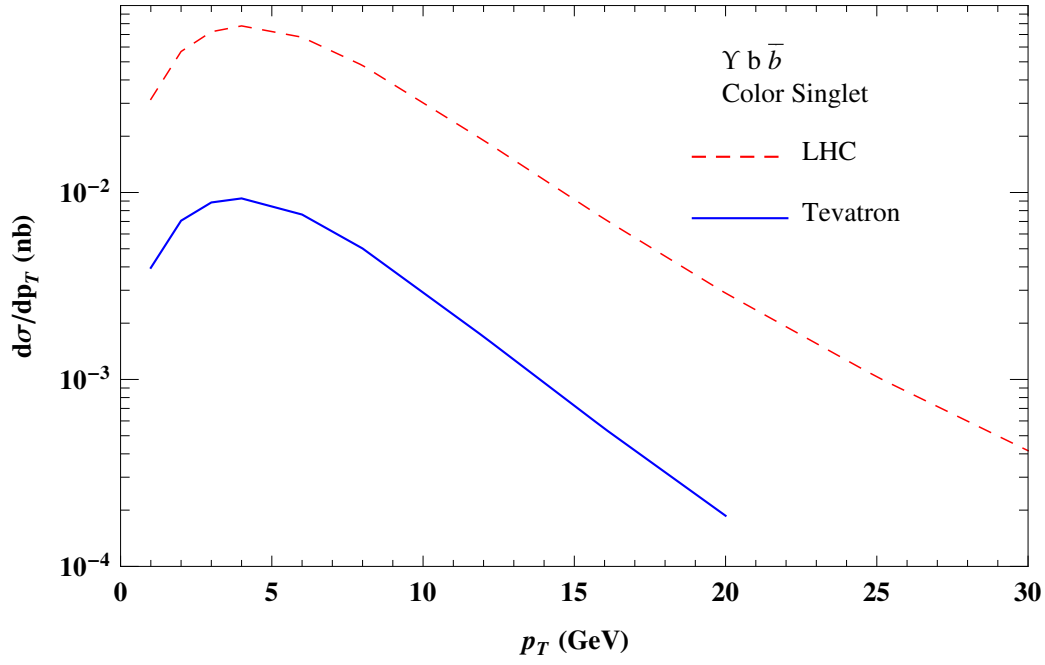
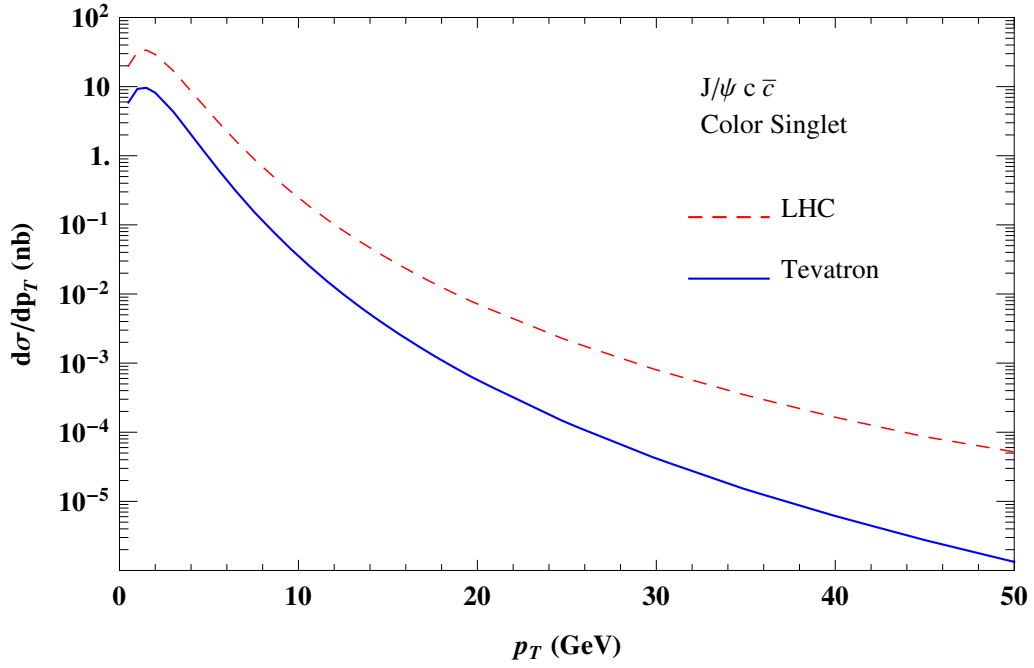


Figure 1: p_T distributions of $J/\psi(\Upsilon)$ production in association with $c\bar{c}(b\bar{b})$ at the Tevatron and LHC. Only color-singlet states are considered.

The readers who are interested in these topics can refer to the corresponding (forthcoming) publications.

Besides the above examples, there are many other aspects of quarkonium physics one can perform analysis with `HELAC-Onia`, for instance, the quarkonium production with jets (inclusive or exclusive⁷) and/or weak bosons. We refrain to illustrate more examples here.

One can feel free to use the modified `PHEGAS`⁸ [42, 7], `RAMBO` [43] or `VEGAS`[44] to perform Monte Carlo evaluation. Standard Les Houches Event files [45] are also generated.

5 Running the program

We are in the position to describe how can one run the program. The program is split in two major phases, which were called *initialization phase* and *computation phase* in Ref.[5]. During the *initialization phase*, the program selects all the relevant sub-amplitudes for the required process and evaluates the color matrix M_{ij} , while during the *computation phase*, it computes the amplitude for each phase space point introduced by `PHEGAS`, `RAMBO` or `VEGAS`.

The running of the program is very easy. If the program is running under the `Unix`, one should specify the `Fortran90` compilation in the first line of `makefile`. The default one is `gfortran`. For the `Windows` user, it is running only after the user has included all of the `Fortran90` files in his/her project. There are two input files that should be specified by the user before running the program. They are `process.inp` and `user.inp`.

In the `process.inp`, the user should tell the program the information of the process including the number of external particles (in the first line) and the ids of the particles (in the second line). The table of the ids for the particles (not hadrons) in the standard-model defined in `HELAC-Onia` are the same as that in `HELAC`, which is shown in Table.7. The naming rules of the ids for the heavy quarkonia in `HELAC-Onia` are:

- (1) The ids of the heavy quarkonia are in 6-digits.
- (2) The first two digits are 44 for charmonia, 55 for bottomonia and 45 for B_c .
- (3) The next four digits are just recording the information of which intermediate Fock states. In general, the four digits are in the order of $(2S + 1)LJc$ for $^{2S+1}L_J^{[c]}$. For example, 3118 means the intermediate state is $^3P_1^{[8]}$.

⁷Thanks to the useful discussion with Qiang Li, we have implemented the matrix element and parton shower matching method MLM scheme [40, 41] in the program for quarkonium associated production with jets. The study of this issue in `HELAC-Onia` will be presented elsewhere.

⁸`PHEGAS` is modified to generate quarkonium events.

$\nu_e, e^-, u, d, \nu_\mu, \mu^-, c, s, \dots$	1, ..., 12
$\bar{\nu}_e, e^+, \bar{u}, \bar{d}, \bar{\nu}_\mu, \mu^+, \bar{c}, \bar{s}, \dots$	-1, ..., -12
γ, Z, W^+, W^-, g	31, ..., 35
H, χ, ϕ^+, ϕ^-	41, ..., 44

Table 7: The ids of the "elementary" particles in the standard model in HELAC-Onia.

- (4) Charmonia and bottomonia are all self-conjugated mesons, while B_c are not. A minus sign is used to represent the anti-particle. In the program, we treat B_c^+ as the particle while B_c^- as the anti-particle. For example, the id of $B_c^-(^3P_1^{[8]})$ is -453118.

Using these rules, one can calculate the helicity amplitudes for S-wave and P-wave quarkonia production from $pp, p\bar{p}$ and e^+e^- collisions. We take one example. If the user want to calculate $gg \rightarrow c\bar{c}[^3P_1^{[8]}] + c\bar{c}$. The first line of `process.inp` is 5, and the second line of `process.inp` is

35 35 443118 7 - 7.

The file `user.inp` is left for the user to specify the parameters in `default.inp` if he/she does not want to use the default values given in `default.inp`⁹. The main parameters are:

- (1) `colpar` represents the type of colliding particles, i.e. 1 for pp , 2 for $p\bar{p}$ and 3 for e^+e^- .
- (2) `energy` is the center-of-mass energy \sqrt{s} in unit of GeV.
- (3) `gener` specifies the Monte Carlo generator, i.e. 0 for PHEGAS, 1 for RAMBO, 2 for DURHAM and 3 for VEGAS, -1 for one phase space point calculation.
- (4) `ranhel` is a parameter to determine whether the program uses the Monte Carlo sampling over the helicity configurations. In specific, if `ranhel`= 0, it does the explicit helicity summation, while if `ranhel`> 0, it does the Monte Carlo sampling. If `ranhel`= 1, the program uses Monte Carlo sampling over the helicities of the "elementary" particles in the standard-model and summing over helicities of quarkonia, while if `ranhel`= 2 it also performs Monte Carlo sampling over ϵ_i^λ for the P-wave

⁹We suggest the user do not change the content in the file `default.inp` unless he/she really knows what he/she is doing.

states, and `ranhel= 3` means it does Monte Carlo sampling over all polarization vectors of heavy quarkonia (of course also over helicities of the "elementary" particles in the standard-model).

- (5) The value of `qcd` determines the amplitudes should be calculated in which theory, i.e. 0 for only electroweak, 1 for electroweak and QCD, 2 for only QCD, 3 for only QED and 4 for QCD and QED.
- (6) `alphasrun` is a parameter to determine whether the strong coupling constant α_s should be running(1) or not(0).
- (7) Flags like `gauge`, `ihiggs` and `widsch` determine the gauge(0 = Feynman gauge, 1 = unitary gauge), whether inclusion Higgs(1) or not(0) and using the fixed(0) or complex(1) scheme for the widths of W^\pm and Z bosons.
- (8) `nmc` is the number of the Monte Carlo iterations.
- (9) `pdf` is the PDF set number proposed in LHAPDF[46]. Entering 0 means no PDF is convoluted.
- (10) `ptdisQ` is a flag whether the p_T distribution of the first final quarkonium are calculated(T) or just total cross section(F). If `ptdisQ` is T, one should also specify which p_T value (`Pt1`) should be calculated.
- (11) `Scale` specifies which renormalization (and PDF factorization) scale should be used. It is explained in the comment line of `default.inp`. If the user chooses the fixed-value scheme, he/she should also supply the value of the scale (`FScaleValue`).
- (12) `exp3pjQ` is a flag whether summing over(F) ${}^3P_J^{[1/8]}$, $J = 0, 1, 2$ or not(T).
- (13) `modes` determines whether the calculated result is the polarized one(1) or not(0). If it is 1, the user should also supply the values of `SDME1` and `SDME2` to let the program know which spin density matrix element to calculate. Meanwhile, the value of `LSJ` represents which "spin" in quarkonium should be specified. The user should also specify the polarization frame (`PolarFrame`).
- (14) The parameters of the physical cuts in calculating the cross sections should also be input by the user if he/she wishes to use his/her values.
- (15) The long distance matrix elements are also supplied in `default.inp`. The user can supply his/her values in `user.inp` with the same format in `default.inp`. The conventions are explained in the comment lines of `default.inp`.

RESULT_eebaretac1ggg.out	sampleebaretac1ggg.lhe
<pre> ... average estimate : 0.373070D-05 +\ 0.200429D-07 variance estimate: 0.401719D-15 +\ 0.559955D-17 out of 100000 100001 points have been used and 100001 points resulted to /= 0 weight whereas 0 points to 0 weight ----- total sigma (nb) = 0.373070D-05 +/- 0.200429D-07 ----- % error: 0.537244D+00 ----- lwri: number of points have used 8931.00000000000000 The Timing Consuming in Phase Space Integration is: 0 h; 4 m; 11 s; 38 centi s </pre>	<pre> <LesHouchesEvents version="1.0"> <!-- File generated with HELAC_PHEGAS_ONIA --> <init> 11 -11 5.300000E+00 5.300000E+00 -1 -1\ -1 -1 3 1 3.7306977547E-03 2.004293\ 5975E-05 1.0000000000E+00 81 </init> <event> ... </pre>

Figure 2: Illustration of output files for $e^-e^+ \rightarrow \eta_c + ggg$ with events generated by PHEGAS.

All other parameters are listed in `default.inp`. The user can fix his/her values in `user.inp` following the format in `default.inp`. Finally, the user just run the program and obtain the result files. In Fig.(2), we give an illustration of the output files for $e^-e^+ \rightarrow \eta_c + ggg$, i.e. `RESULT_eebaretac1ggg.out` and `sampleebaretac1ggg.lhe`¹⁰. At the end of the first output file, the total cross section is shown in the circle as well as the numerical error, while in the second file is just the event information of the considered process.

6 Summary and outlooks

The exploitation of the fundamental law in the nature is the main aim of the running of the LHC. Heavy quarkonium, which is one type of the simplest hadrons, provides an ideal laboratory to test and understand QCD. The discrepancies between the experimental measurements and the theoretical predictions imply that we still do not understand the production mechanism of the heavy quarkonium. Moreover, the quarkonia like J/ψ and Υ production at the LHC will not only be taken as calibration tools but also be very useful for TeV physics and even new physics. Hence, it is mandatory to improve the reliability

¹⁰Note that Les Houches Event files can only be generated via PHEGAS in HELAC-Onia now.

of Monte Carlo simulation. From the present theoretical studies, the radiative corrections are very indispensable even at qualitative level to the quarkonium production.

Unlike the case in parton-level, the automatic tools for calculating quarkonium helicity amplitudes are still rare on the market. In this presentation, we have achieved the first step to the development of an automatic Monte Carlo generator for heavy quarkonium. Our program is an extension of the present published HELAC [5, 6, 7], which is based on an off-shell recursive algorithm or Dyson-Schwinger equations. We dubbed it as HELAC-Onia. It provides an automatic computation tool for heavy quarkonium helicity amplitudes in the standard model with high efficiency. We have also shown the applications of our tool to the various aspects of the heavy quarkonium production from $pp, p\bar{p}$ and e^+e^- collisions.

The following steps are to realize the automation of the next-to-leading order quarkonium helicity amplitudes computations. With such a code, one can perform the analysis of the heavy quarkonium production at a full next-leading order level, which is much more reliable and useful especially at the LHC.

Acknowledgements

This work was supported in part by the National Natural Science Foundation of China (Nos.11021092, and 11075002), and the Ministry of Science and Technology of China (No.2009CB825200). First of all, we are grateful to Costas Papadopoulos, Malgorzata Worek and the HELAC team to allow us using the acronym and encourage us to upload the program on the HELAC web-page. We would also like to thank Prof. Kuang-Ta Chao for providing important supports on this project, Qiang Li for useful discussion on matrix element and parton shower matching and Pierre Artoisenet for using MADONIA.

References

- [1] G. T. Bodwin, E. Braaten, and G. Lepage, “Rigorous QCD analysis of inclusive annihilation and production of heavy quarkonium,” *Phys.Rev.* **D51** (1995) 1125–1171, hep-ph/9407339.
- [2] G. T. Bodwin, “Theory of Charmonium Production,” 1208.5506.
- [3] P. Artoisenet, F. Maltoni, and T. Stelzer, “Automatic generation of quarkonium amplitudes in NRQCD,” *JHEP* **0802** (2008) 102, 0712.2770. 17 pages, 7 figures.
- [4] J.-X. Wang, “Progress in FDC project,” *Nucl.Instrum.Meth.* **A534** (2004) 241–245, hep-ph/0407058.
- [5] A. Kanaki and C. G. Papadopoulos, “HELAC: A package to compute electroweak helicity amplitudes,” *Comput. Phys. Commun.* **132** (2000) 306–315, hep-ph/0002082.
- [6] C. Papadopoulos and M. Worek, “HELAC - A Monte Carlo generator for multi-jet processes,” hep-ph/0606320.
- [7] A. Cafarella, C. G. Papadopoulos, and M. Worek, “Helac-Phegas: a generator for all parton level processes,” *Comput. Phys. Commun.* **180** (2009) 1941–1955, 0710.2427.
- [8] P. Artoisenet, J. M. Campbell, J. Lansberg, F. Maltoni, and F. Tramontano, “ Υ Production at Fermilab Tevatron and LHC Energies,” *Phys.Rev.Lett.* **101** (2008) 152001, 0806.3282.
- [9] F. Dyson, “The S matrix in quantum electrodynamics,” *Phys.Rev.* **75** (1949) 1736–1755.
- [10] J. S. Schwinger, “On the Green’s functions of quantized fields. 1.,” *Proc.Nat.Acad.Sci.* **37** (1951) 452–455.
- [11] J. S. Schwinger, “On the Green’s functions of quantized fields. 2.,” *Proc.Nat.Acad.Sci.* **37** (1951) 455–459.
- [12] F. A. Berends and W. T. Giele, “Recursive Calculations for Processes with n Gluons,” *Nucl. Phys.* **B306** (1988) 759.

- [13] F. Caravaglios and M. Moretti, “An algorithm to compute Born scattering amplitudes without Feynman graphs,” *Phys. Lett.* **B358** (1995) 332–338, hep-ph/9507237.
- [14] G. ’t Hooft, “A Planar Diagram Theory for Strong Interactions,” *Nucl.Phys.* **B72** (1974) 461.
- [15] A. Kanaki and C. G. Papadopoulos, “HELAC-PHEGAS: Automatic computation of helicity amplitudes and cross-sections,” hep-ph/0012004.
- [16] F. Maltoni, K. Paul, T. Stelzer, and S. Willenbrock, “Color flow decomposition of QCD amplitudes,” *Phys.Rev.* **D67** (2003) 014026, hep-ph/0209271.
- [17] A. Petrelli, M. Cacciari, M. Greco, F. Maltoni, and M. L. Mangano, “NLO production and decay of quarkonium,” *Nucl.Phys.* **B514** (1998) 245–309, hep-ph/9707223.
- [18] B. Guberina, J. H. Kuhn, R. D. Peccei and R. Ruckl, “Rare Decays of the Z0,” *Nucl.Phys.* **B 174**, 317 (1980).
- [19] E. L. Berger and D. L. Jones, “Inelastic Photoproduction of J/psi and Upsilon by Gluons,” *Phys.Rev.* **D23** (1981) 1521–1530.
- [20] Y.-Q. Ma, K. Wang, and K.-T. Chao, “J/psi (psi’) production at the Tevatron and LHC at $O(\alpha_s^4 v^4)$ in nonrelativistic QCD,” *Phys.Rev.Lett.* **106** (2011) 042002, 1009.3655.
- [21] M. Butenschoen and B. A. Kniehl, “Reconciling J/ψ production at HERA, RHIC, Tevatron, and LHC with NRQCD factorization at next-to-leading order,” *Phys.Rev.Lett.* **106** (2011) 022003, 1009.5662.
- [22] M. Butenschoen and B. A. Kniehl, “J/psi polarization at Tevatron and LHC: Nonrelativistic-QCD factorization at the crossroads,” *Phys.Rev.Lett.* **108** (2012) 172002, 1201.1872.
- [23] K.-T. Chao, Y.-Q. Ma, H.-S. Shao, K. Wang, and Y.-J. Zhang, “ J/ψ polarization at hadron colliders in nonrelativistic QCD,” *Phys.Rev.Lett.* **108** (2012) 242004, 1201.2675.
- [24] B. Gong, L.-P. Wan, J.-X. Wang, and H.-F. Zhang, “Polarization for Prompt J/psi, psi(2s) production at the Tevatron and LHC,” 1205.6682.

- [25] M. Butenschoen and B. A. Kniehl, “Complete next-to-leading-order corrections to J/ψ photoproduction in nonrelativistic quantum chromodynamics,” *Phys.Rev.Lett.* **104** (2010) 072001, 0909.2798.
- [26] M. Butenschoen and B. A. Kniehl, “Probing nonrelativistic QCD factorization in polarized J/ψ photoproduction at next-to-leading order,” 1109.1476.
- [27] C.-H. Chang, C. Driouichi, P. Eerola, and X. G. Wu, “BCVEGPY: An Event generator for hadronic production of the B_c meson,” *Comput.Phys.Commun.* **159** (2004) 192–224, hep-ph/0309120.
- [28] C.-H. Chang, J.-X. Wang, and X.-G. Wu, “BCVEGPY2.0: A Upgrade version of the generator BCVEGPY with an addendum about hadroproduction of the P-wave $B(c)$ states,” *Comput.Phys.Commun.* **174** (2006) 241–251, hep-ph/0504017.
- [29] A. Berezhnoy, V. Kiselev, and A. Likhoded, “NonAbelian nature of asymmetry for the $B(c)$ meson production in gluon photon interaction,” *Phys.Atom.Nucl.* **61** (1998) 252–259, hep-ph/9710429.
- [30] J. Pumplin, D. Stump, J. Huston, H. Lai, P. M. Nadolsky, *et al.*, “New generation of parton distributions with uncertainties from global QCD analysis,” *JHEP* **0207** (2002) 012, hep-ph/0201195.
- [31] N. Brambilla, S. Eidelman, B. Heltsley, R. Vogt, G. Bodwin, *et al.*, “Heavy quarkonium: progress, puzzles, and opportunities,” *Eur.Phys.J.* **C71** (2011) 1534, 1010.5827.
- [32] K.-Y. Liu, Z.-G. He, and K.-T. Chao, “Inclusive charmonium production via double $c\bar{c}$ in e^+e^- annihilation,” *Phys.Rev.* **D69** (2004) 094027, hep-ph/0301218.
- [33] E. Braaten and J. Lee, “Exclusive double charmonium production from e^+e^- annihilation into a virtual photon,” *Phys.Rev.* **D67** (2003) 054007, hep-ph/0211085.
- [34] G. T. Bodwin, J. Lee, and E. Braaten, “Exclusive double charmonium production from e^+e^- annihilation into two virtual photons,” *Phys.Rev.* **D67** (2003) 054023, hep-ph/0212352.
- [35] R. Li, Y.-J. Zhang, and K.-T. Chao, “Pair Production of Heavy Quarkonium and $B(c)^{(*)}$ Mesons at Hadron Colliders,” *Phys.Rev.* **D80** (2009) 014020, 0903.2250.

- [36] P. Artoisenet, J. Lansberg, and F. Maltoni, “Hadroproduction of J/ψ and ν in association with a heavy-quark pair,” *Phys.Lett.* **B653** (2007) 60–66, hep-ph/0703129. 13 pages, 5 figures.
- [37] H.-S. Shao and K.-T. Chao, “Spin correlations in polarizations of P-wave charmonia χ_{cJ} and impact on J/ψ polarization,” 1209.4610.
- [38] K.-T. Chao, Y.-Q. Ma, H.-S. Shao, and K. Wang, “Polarizations of χ_{c1} and χ_{c2} inclusive production at the LHC,” XXXX.XXXX.
- [39] H.-S. Shao and K.-T. Chao, “Polarized χ_c Production in Association with A Charm Quark Pair at The LHC,” XXXX.XXXX.
- [40] M. L. Mangano, M. Moretti, F. Piccinini, and M. Treccani, “Matching matrix elements and shower evolution for top-quark production in hadronic collisions,” *JHEP* **0701** (2007) 013, hep-ph/0611129.
- [41] J. Alwall, S. Hoche, F. Krauss, N. Lavesson, L. Lonnblad, *et al.*, “Comparative study of various algorithms for the merging of parton showers and matrix elements in hadronic collisions,” *Eur.Phys.J.* **C53** (2008) 473–500, 0706.2569.
- [42] C. G. Papadopoulos, “PHEGAS: A phase space generator for automatic cross-section computation,” *Comput. Phys. Commun.* **137** (2001) 247–254, hep-ph/0007335.
- [43] R. Kleiss, W. Stirling, and S. Ellis, “A NEW MONTE CARLO TREATMENT OF MULTIPARTICLE PHASE SPACE AT HIGH-ENERGIES,” *Comput.Phys.Commun.* **40** (1986) 359.
- [44] G. Lepage, “A New Algorithm for Adaptive Multidimensional Integration,” *J.Comput.Phys.* **27** (1978) 192. Revised version.
- [45] E. Boos, M. Dobbs, W. Giele, I. Hinchliffe, J. Huston, *et al.*, “Generic user process interface for event generators,” hep-ph/0109068.
- [46] M. Whalley, D. Bourilkov, and R. Group, “The Les Houches accord PDFs (LHAPDF) and LHAGLUE,” hep-ph/0508110.